Stem Cell Research (2011) 6, 13–22

available at www.sciencedirect.com

www.elsevier.com/locate/scr

REGULAR ARTICLE

Human embryonic stem cells and derived contractile embryoid bodies are susceptible to Coxsakievirus B infection and respond to interferon Iβ treatment

María E. Scassa[a], Carolina Jaquenod de Giusti[b], María Questa[a], Gabriela Pretre[b], Guillermo A. Videla Richardson[a], Carolina Bluguermann[a], Leonardo Romorini[a], María F. Ferrer[b], Gustavo E. Sevlever[a], Santiago G. Miriuka[a,*], Ricardo M. Gómez[b,*]

[a] *Laboratorio de Biología del Desarrollo Celular, FLENI, Buenos Aires, Argentina*
[b] *Instituto de Biotecnología y Biología Molecular, CCT-La Plata, Argentina*

Received 12 April 2010; received in revised form 5 September 2010; accepted 10 September 2010

Abstract We studied the susceptibility of human embryonic stem cells and derived contractile embryoid bodies from WAO9, HUES-5 and HUES-16 cell lines to Coxsackievirus B infection. After validating stem cell-like properties and cardiac phenotype, Coxsackievirus B receptors CAR and DAF, as well as type I interferon receptors were detected in all cell lines and differentiation stages studied. Real-time PCR analysis showed that CAR mRNA levels were 3.4-fold higher in undifferentiated cells, while DAF transcript levels were 2.78-fold more abundant in differentiated cultures ($P<0.05$). All cell lines were susceptible to Coxsackievirus serotypes B1-5 infection as shown by RT-PCR detection of viral RNA, immunofluorescence detection of viral protein and infectivity titration of cell culture supernatants resulting in cell death. Supernatants infectivity titers 24-48 h post-infection ranged from 10^5-10^6 plaque forming units (PFU)/ml, the highest titers were detected in undifferentiated cells. Cell viability detected by a colorimetric assay, showed inverse correlation with infectivity titers of cell culture supernatants. Treatment with 100 U of interferon Iβ significantly reduced viral replication and associated cell death during a 24–48 h observation period, as detected by reduced infectivity titers in the supernatants and increased cell viability by a colorimetric assay, respectively. We propose human embryonic stem cell and derived contractile embryoid bodies as a valid model to study cardiac Coxsackievirus B infection.

Introduction

Human embryonic stem cells (hESC) are derived from the inner cell mass of an early embryo and possess a unique developmental potential. They are defined as pluripotent because of their capacity to differentiate into all cell lineages present in embryonic tissue. In addition, hESC can self-renew and be cultured indefinitely *in vitro*. Because hESC have been shown to undergo robust *in vitro* differentiation, these cells may be

* Corresponding authors. S.G. Miriuka is to be contacted at Departamento de Cardiología, FLENI, Montañeses 2325 – (C1428AQK) Buenos Aires, Argentina. R.M. Gómez, IBBM, CONICET-UNLP, calle 49 y 115, 1900 La Plata, Argentina. Fax: +54 221 422 9777.
E-mail addresses: smiriuka@fleni.org.ar (S.G. Miriuka), rmg@biol.unlp.edu.ar (R.M. Gómez).

1873-5061/$ – see front matter © 2010 Elsevier B.V. All rights reserved.
doi:10.1016/j.scr.2010.09.002

considered a powerful tool to explore different events affecting cardiac cells (Lev et al., 2005), including molecular pathogenesis and drug and toxicology testing (Steel et al., 2009; Reppel et al., 2007). The development of induced pluripotent stem cells (iPS) expands these possibilities further, since it is now possible to study cardiomyocytes derived from reprogrammed somatic cells of patients with cardiac disease (Yokoo et al., 2009; Zhang et al., 2009).

Coxsackieviruses B (CVB), which include 6 serotypes, are human enteroviruses belonging to the *Picornaviridae* family (Pallansch and Roos, 2001). Together with CVA9 and the echoviruses (EV), CVB are currently classified as type B Enteroviruses (Stanway et al., 2004), interacting with at least two receptor proteins present on the cytoplasmic membrane. All CVB, as well as some adenoviruses, recognize and enter the cell through the coxsackievirus-adenovirus receptor (CAR), which is a 46-kDa protein belonging to the immunoglobulin supergene family (Bergelson et al., 1997). Although viral uncoating is initiated only by CAR interactions (Milstone et al., 2005), some CVB interact with an additional 70-kDa molecule known as the decay-accelerating factor (DAF, also known as CD55), which is a surface-expressed complement regulatory protein (Shafren et al., 1995). With the exception of CVB6, all CVB serotypes are expected to produce similar diseases (Pallansch and Roos, 2001); nevertheless, most experimental studies have been performed with CVB3 because some viral variants may induce myocarditis in animal models (Tracy and Gauntt, 2008). CVB1 was the predominant enterovirus circulating in the US during 2007 (Anon, 2008), and viruses derived from an infectious clone (Iizuka et al., 1991) have been used in several studies (Rinehart et al., 1997; Zhong et al., 2008).

Although CVB are a frequent cause of subclinical infection, they may also cause other diseases such as viral myocarditis (Pallansch and Roos, 2001), symptoms of which may be seen either shortly after acute infection potentially triggering severe myocardial dysfunction, or during the chronic phase of disease resulting in dilated cardiomyopathy (DCM) (Feldman and McNamara, 2000; Yajima and Knowlton, 2009). Serological data initially suggested a link between viral myocarditis and DCM but with the exception of some pediatric cases, it was almost impossible to detect infectious virus in cardiac tissue samples from necropsies or biopsies. More recently, with the aid of molecular procedures, multiple studies have detected viral RNA (Feldman and McNamara, 2000; Ellis and Di Salvo,

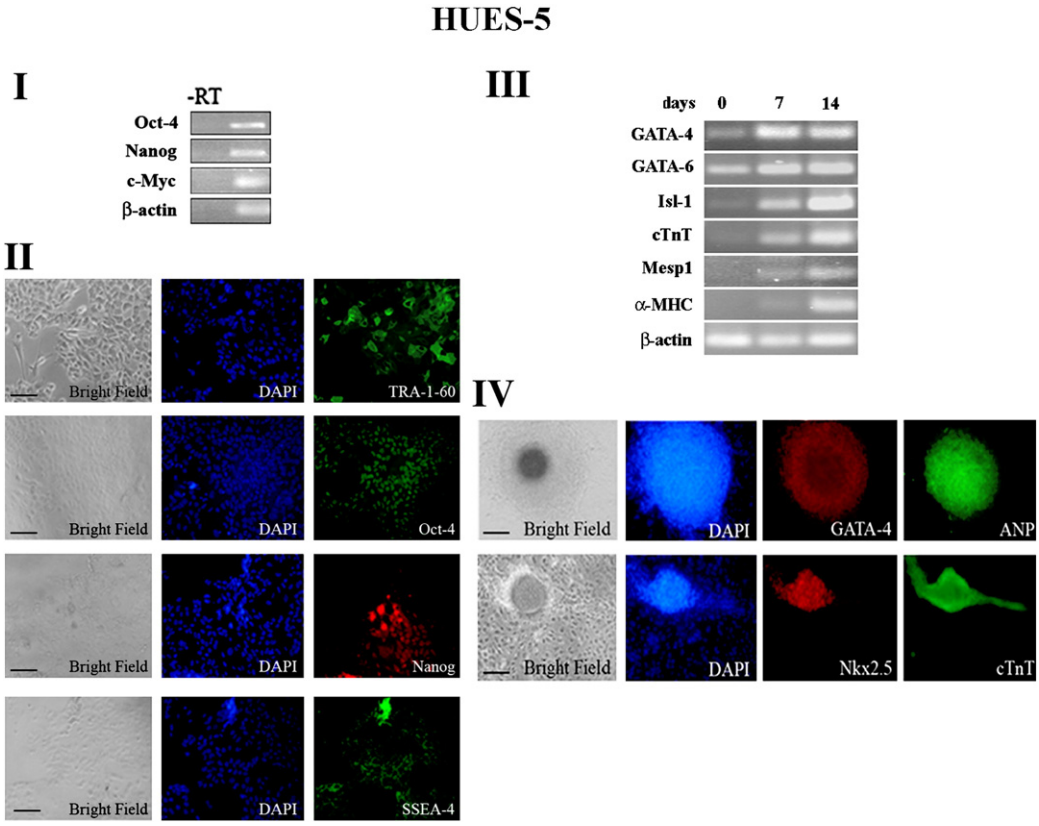

Figure 1 Expression of stem cell and cardiac markers in hESC at different stages of differentiation. (I) RT-PCR analysis of stem cell-like transcripts was performed on the undifferentiated HUES-5 cells. (II) The HUES-5 hESC were grown on a Matrigel™ coated surface for 3 days and then fixed and stained with primary antibodies recognizing stem cell markers. The figure shows representative images of hESC stained with TRA-1-160, Oct-4, Nanog and SSEA-4. (III) Semiquantitative RT-PCR of cardiac-like transcripts was performed for hESC at different stages of differentiation; β-actin was used as a loading control (I and III). (IV) Immunofluorescence staining of hESC at 14 days after the onset of differentiation. The figure shows representative images of contractile EB stained with primary antibodies for GATA-4, ANP, Nkx2.5 and cTnT. The nuclei were counterstained with DAPI. The scale bars represent 100 μm. Abbreviations: TRA-1-60, Tumor Rejection Antigen 1-60; Oct-4, Octamer 4; SSEA-4, Stage-Specific Embryonic Antigen; ANP, atrial natriuretic peptide; cTnT, cardiac troponin T; Mesp1, mesoderm posterior factor 1; Isl-1, Islet-1; α-MHC, α-myosin heavy chain.

2007) or viral proteins (Li et al., 2000) in heart tissue samples from patients with acute viral myocarditis or DCM. Currently, CVB are accepted as one of the most frequent viruses involved in heart infections (Feldman and McNamara, 2000). At the present time, no specific treatment is recommended for viral myocarditis (Feldman and McNamara, 2000), although type I interferon (IFN-I) has been recently administered to patients in the chronic phase of the infection (Kuhl et al., 2003), as well as in *ex vivo* (Kandolf et al., 1985) and *in vivo* models of viral myocarditis (Deonarain et al., 2004). In all of these studies, IFN-I administration has shown promising results.

In this study, we show that both hESC and hESC-derived contractile embryoid bodies (hESC-EB) from three different cell lines express both CAR and DAF receptor transcripts and proteins, as well as the interferon-α/β receptor α chain 1 (IFNAR1) and IFNAR2 transcripts. We also found that all cells were susceptible to infection by the CVB1-5 strains. In addition, IFN-Iβ treatment reduced CVB-induced cell lysis and replication. We propose that hESC and hESC-EB as valid *ex vivo* models for the study different aspects of CVB infection of the heart.

Results

Analysis of stem cell and cardiac marker expression in hESC and hESC-EB

We first validated the pluripotent nature of the hESC lines used in this study by RT-PCR and immunofluorescence (IF) microscopy. As shown in Fig. 1-I, undifferentiated hESC expressed transcripts associated with pluripotency such as Oct-4, Nanog and c-Myc. These cells also exhibited robust expression of stem cell associated markers TRA1-60, Oct-4, Nanog and SSEA-4 (Fig. 1-II) , thus indicating that under these experimental conditions, hESC lines had retained self renewal properties without visible differentiation.

Next, differentiation of hESC was induced using an EB-based approach. On day 8, (after 7 days in suspension followed by 1 day of outgrowth in gelatin-coated dishes) we observed formation of contracting regions, increasing in number thereafter. The proportion of contractile EB differed among the hESC lines (HUES-5: 17.7±3.2%; WA-09: 8.9±2.5% and HUES-16: 3±0.5%), beating spontaneously at an average frequency of 29±7.3 beats/min. This rate increased 49±6.2% compared to the baseline after incubation with 10 nM of norepinephrine (NE). To confirm the EB had acquired a cardiac phenotype, RT-PCR and IF analyses were performed. Mesoderm expression (mesoderm posterior factor-1, Mesp1), cardiac mesoderm (GATA-4, GATA-6, Nkx2.5, Islet-1) and cardiomyocyte associated genes (atrial natriuretic peptide, ANP; cardiac Troponin T, cTnT and α-myosin heavy chain, α-MHC) was assessed 7 and 14 days after the onset of differentiation (Fig. 1-III and IV). These results demonstrate that the hESC had effectively differentiated into EB-containing cardiomyocytes *in vitro*.

hESC and hESC-EB express CAR, DAF and IFN-I receptors

Next, we evaluated the expression of CVB and IFN-I receptors in both the hESC and hESC-EB. To avoid contamination of

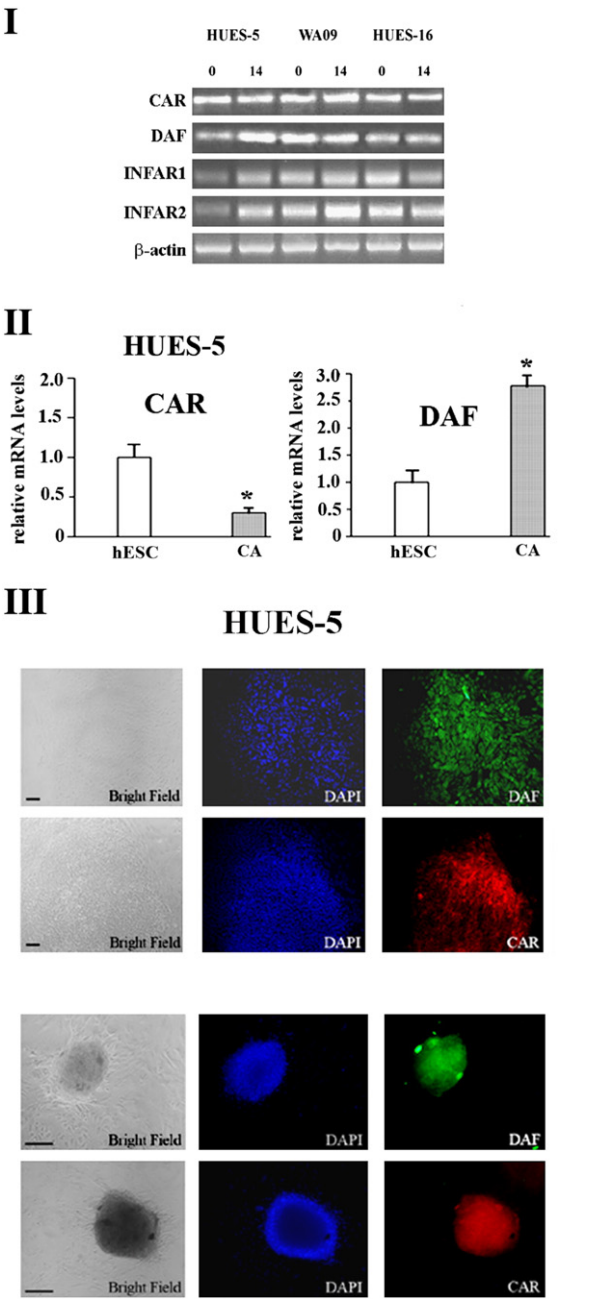

Figure 2 Expression of key molecules that mediate viral infection (I) Semiquantitative RT-PCR was performed on the HUES-5, WA09 and HUES-16 at 0 and 14 days of differentiation; β-actin was used as a loading control. (II) Immunofluorescence staining of HUES-5, WA09 and HUES-16 at 0 and 14 days of differentiation. The figure shows representative images of HUES-5 undifferentiated colonies (top panel) and EB (bottom panel) stained for CAR and DAF. The nuclei were counterstained with DAPI. The scale bars represent 100 μm. (III) Real-time RT-PCR analysis of CAR and DAF mRNA levels in HUES-5 in hESC and contractile areas of EB. The **GAPDH** mRNA expression level was used **to normalize the** expression data. Each bar represents the mean ± SEM of three independent experiments. A paired Student's *t* test was used to compare undifferentiated and differentiated samples (*$P<0.05$). Abbreviations: CA, contractile areas; CAR, coxsackievirus-adenovirus receptor; DAF, decay-accelerating factor; IFNAR1, human interferon-α/ß receptor α chain 1; IFNAR2, human interferon-α/β receptor α chain 2.

cultures by mouse embryonic fibroblasts (MEF), hESC were grown in feeder cell-free conditions (Matrigel™ coated dishes and conditioned medium) for at least four passages prior to cell harvest or viral infection. RT-PCR studies for CVB and IFN-I receptors showed that all hESC lines studied expressed the aforementioned molecules during both the undifferentiated and differentiated stages (Fig. 2-I). Because the HUES-5 cell line had the highest proportion of beating EB it was selected for used in the subsequent studies. The presence of both viral receptors was further confirmed by IF studies (Fig. 2-II). To analyze the expression levels of CAR and DAF, real-time RT-PCR analysis was performed. The results show that the transcript level of CAR was 3.40 ± 0.31 fold higher in undifferentiated cells, while the DAF mRNA level was 2.78 ± 0.28 fold higher in the differentiated cells (Fig. 2-III) ($P<0.05$).

CVB replicates in several hESC lines and hESC-EB

To evaluate the susceptibility of hESC and hESC-EB to CVB infection, the cells were infected with CVB serotypes 1-5. In hESC, a cytopathic effect (cpe), characterized by ballooning, detachment and cell death was observed 12 h post-infection (pi) and reached 80% of the monolayer at 24 h pi (Fig. 3-I and IV). In the hESC-EB, a similar result was observed (Fig. 3-II), although it was delayed because contractile areas stop beating 48 h pi, later followed by cell lysis (supplementary data). A few fibroblast-like cells did not show any cpe and remained viable. The viral infectivity titration of supernatants ranged between 10^5 to 10^6 PFU/ml. Higher titers were detected in undifferentiated cells (≅1 log), no significant differences were found between cell lines or viral strains (Fig. 3-III). Cell viability was evaluated using a XTT/PMS vital dye assay. As shown in Fig. 3-IV 20% of hESC or hESC-EB remained viable 24 or 48 h after CVB3 1/10 infection, respectively. As expected, an increase in cell viability was observed when 10-fold serial dilutions of CVB3 were used. Viral replication was further confirmed by detection of the viral RNA by RT-PCR and immunostaining of viral protein 1 (VP1) in hESC (Fig. 4-I left panel and II) and EB (Fig. 4-I right panel and III). Thus, we have shown that both undifferentiated hESC and hESC-derived contractile EB are susceptible to a productive CVB infection.

Human IFN-Iβ inhibited CVB replication

To determine whether IFN-Iβ treatment inhibited CVB replication, hESC and hESC-EB cultures were treated with 100 U of recombinant human IFN-Iβ 24 h prior to viral infection. No changes in cell morphology or viability were observed in cell culture media containing IFN-Iβ 100 U or less. However, with 500 U some alteration in cell morphology was observed, (data not shown). These results indicated untreated hESC exhibited cpe changes throughout the monolayer or the beating area of EB, while IFN-Iβ treated cells were protected from viral-induced lysis (Fig. 5-I and II, respectively). Moreover, these findings correlated with a decline in viral titers (>1 log) in culture supernatants at 24 (hESC) or 48 h (hESC-EB), and with a dose-dependent an increase in cell viability (Fig. 5-III and IV, respectively). Importantly, when the hESC-EB were treated with IFN-Iβ they retained their contractile activity for 48 h pi, whereas the untreated EB stopped beating (supplementary data).

Discussion

Although murine embryonic stem cells have been cultured for almost twenty years, culture conditions for hESC remained elusive, and it took researchers a much longer time to define these complex conditions. Human embryonic stem cells were discovered a decade ago, after Thomson and co-workers developed a culture system able to maintain hESC indefinitely in an undifferentiated state (Thomson et al., 1998). In recent years, multiple protocols have been developed to produce various adult cells *in vitro*. Kehat *et al*. were the first to demonstrate that hESC can differentiate into cardiomyocytes (Kehat et al., 2001). Multiple publications thereafter proved these cells were mature cardiomyocytes, as defined by their gene and protein expression, as well as their physiological properties (He et al., 2003; Xu et al., 2002). Even though hESC-derived cardiomyocytes probably retain features related to their fetal origin; they are nevertheless mature enough to beat spontaneously and to respond to cell surface signals, such as incubation with NE which rapidly increases their beating rate.

Relatively few studies have evaluated CAR expression in hESC, although a recent paper reported striking variation in adenovirus infection rates among different hESC lines, correlating with CAR expression (Brokhman et al., 2009), the three cell lines studied in this paper, WAO9, HUES-5 and HUES-16, expressed CAR at similar levels. This difference may perhaps have due to differences in cell lines or culture conditions used. However, CAR transcript was always more abundant in hESC than in hESC-EB, a finding in agreement with expression levels found in embryos and adult heart tissue (Freimuth et al., 2008). Interestingly, CAR has been reported to be highly expressed in the hearts of DCM patients, and it has been suggested that these patients may be more susceptible to heart CVB infection (Noutsias et al., 2001). As for DAF, a protein present on the surface of normal cardiomyocytes (Zimmermann et al., 1990), cognate

Figure 3 Coxsackievirus B variants replicated and induced cytopathic changes in both hESC and hESC-EB. The figure shows representative images of (I) hESC (HUES-5, WA09 and HUES-16) colonies 24 h pi, and (II) hESC-EB at day 14 of differentiation, 48 h pi. The scale bars represent 200 μm. Abbreviations: CVB1, Coxsackievirus subgroup B, serotype 1 and CVB3, Coxsackievirus subgroup B, serotype 3. (III) Infectivity titration of infected cell supernatant performed with 100 μl of 10-fold serial dilutions in a plaque forming unit (PFU) assay at 24 (hESC) or 48 h pi (hESC-EB). Each bar represents the mean ± SEM of three independent experiments. Similar results were observed after infection with CVB2, CVB4 or CVB5. (IV) Cell viability was measured by using the XTT/PMS vital dye assay at 24 h pi of hESC or 48 h pi of contractile EB using 10^{-1} to 10^{-3} serial dilutions of CVB3. Each bar represents the mean ± SEM of two independent experiments (*$P<0.05$).

mRNA was also expressed at similar levels in all three cell lines studied. But, in contrast to CAR, mRNA levels were higher in EB than in undifferentiated cells.

Both CAR and DAF have been implicated in CVB infection. Molecular events underlying CVB entry have been described for polarized (Coyne and Bergelson, 2006) and nonpolarized cells

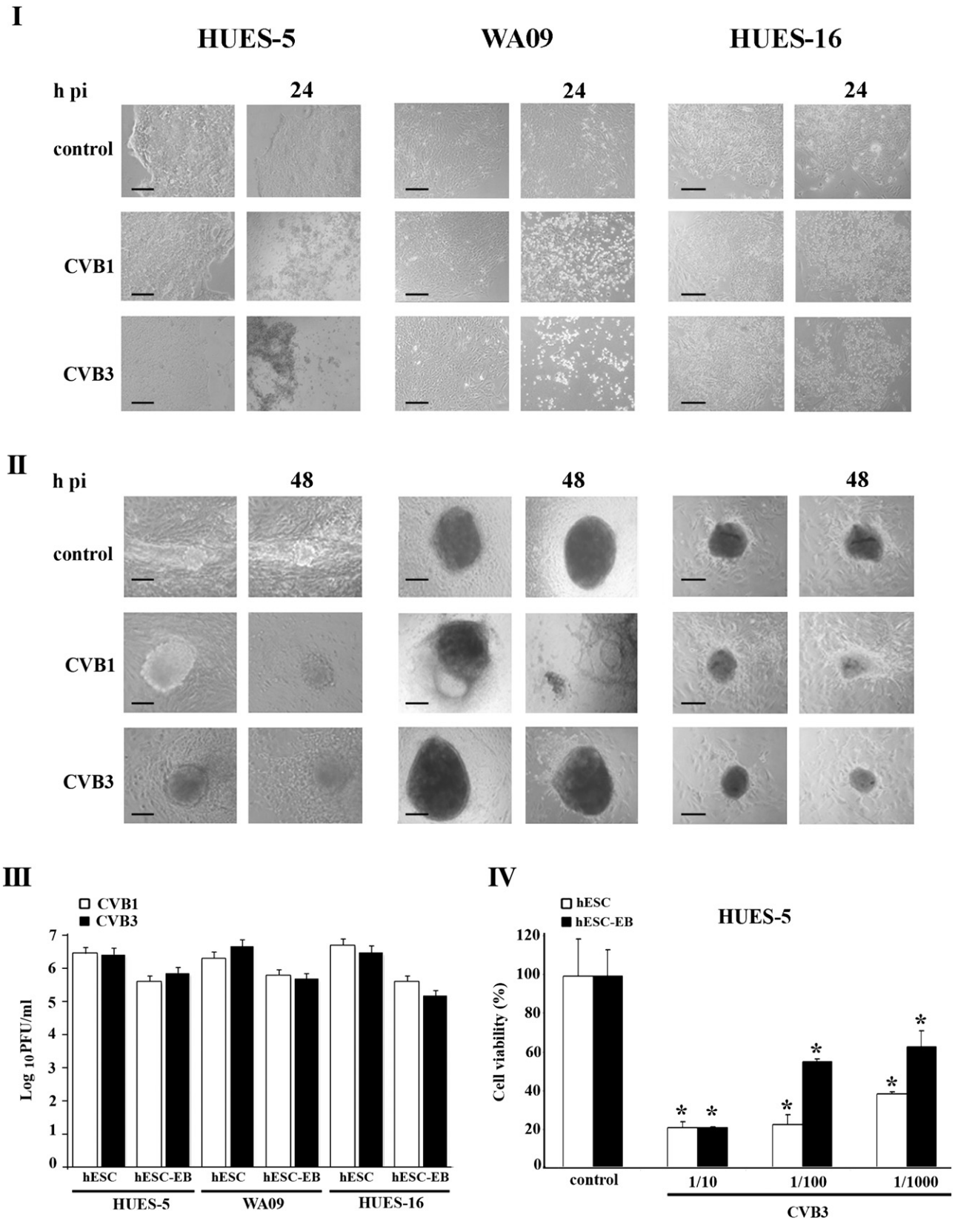

(Patel et al., 2009). However, the exact mechanism involved in CVB infection of cardiomyocytes is unknown. Moreover, some aspects of infection could be specific to human cells. For example, CVB can interacts with human and murine CAR. However, unlike human DAF, CVB does not bind to rodent DAF protein analogues (Spiller et al., 2000) precluding use of a suitable rodent model. Additionally, design of a human *in vitro* model system has been hindered by difficulties associated with culturing human cardiomyocytes derived from adult heart tissues as well as by low availability of cardiac cell cultures from fetal sources (Kandolf et al., 1985). The emergence of embryonic stem cells and protocols for cardiomyocyte differentiation has allowed modern research to overcome these problems. After testing our cell lines for the presence of viral receptors, we subsequently assessed the susceptibility of these cell lines to CVB infection. Pioneer work by Feuer *et al.* performed in mice revealed CVB3 preferentially targets proliferating neural stem cells located in the neonatal central nervous system (Feuer et al., 2003, 2005). In our study, we extended these observations showing both hESCs and hESC-EB presented susceptibility to CVB infection. Several lines of evidence suggest host cell status may play a key role in determining CVB infection outcome. In this regard, proliferation appears to favour productive CVB infection (Tabor-Godwin et al., 2010), and perhaps also contribute to CVB enhanced replication observed in hESC compared to hESC-EB.

The data presented herein agree with previous studies performed with cardiomyocytes derived from human fetal tissue (Kandolf et al., 1985) or newborn mice (Gomez et al., 1993). We also show that IFN-Iβ administration prior to infection was able to reduce viral replication and subsequent cell death. This cytokine was chosen because previous published reports have shown IFN-Iβ treatment eliminates cardiotropic viruses, improving left ventricular function in patients with myocardial persistence of viral genomes and left ventricular dysfunction (Kuhl et al., 2003). Although clinical trials with IFN are still in progress, the results seem promising (Matsumori, 2007). The model described here is novel, relatively simple and can be easily reproduced in any laboratory currently working on hESC. Our findings suggest this model can be useful for the evaluation of potential drug therapies for viral myocarditis.

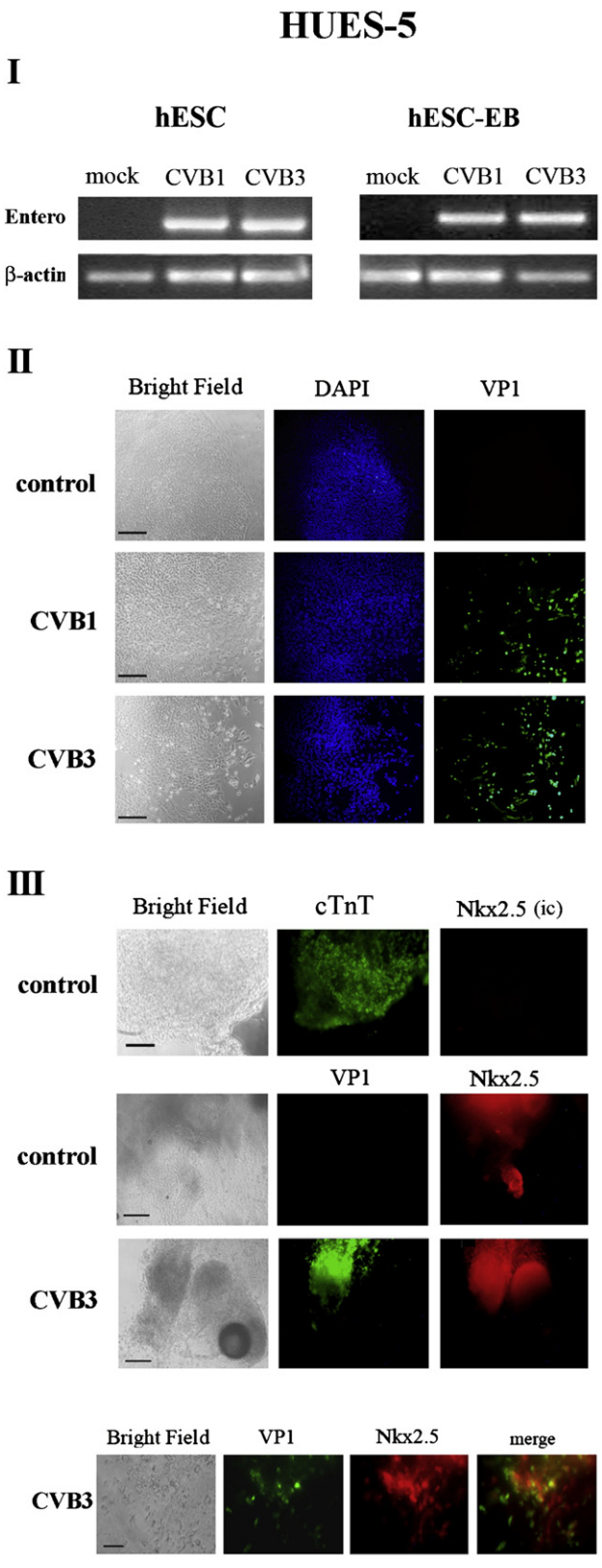

Figure 4 Intracellular presence of viral RNA and VP1 protein. (I) RT-PCR of total RNA obtained from hESC and contractile areas of EB performed at 8 or 48 h pi, respectively in order to determine the presence of CVB1 or CVB3 RNA. Mock (uninfected control cells). β-actin was used as positive control. (II) The figure shows representative images of undifferentiated HUES-5 colonies 8 h pi with CVB1 and CVB3 stained for VP1. The nuclei were counterstained with DAPI. The scale bars represent 200 μm. (III) hESC-EB at day 14 of differentiation and 48 h pi were stained for VP1 and Nkx2.5 (middle and bottom panels). A representative contractile EB was stained for cTnT and simultaneously used for rabbit IgG isotype control (ic)(top panel). The scale bars represent 100 μm. A merged image of a representative contractile area stained with VP1 and Nkx2.5 (bottom panel) is shown. The scale bars represent 50 μm. Abbreviations: VP1, Viral Protein 1; CVB1, Coxsackievirus subgroup B, serotype 1; CVB3, Coxsackievirus subgroup B, serotype 3. Similar results were observed when undifferentiated or differentiated cells were infected with CVB2, CVB4 or CVB5.

Conclusions

In conclusion, we used hESC and hESC-EB to analyze the presence of specific cell markers, such as CVB and IFN-I receptors. Additionally cell susceptibility to CVB infection was analyzed by titrating supernatant infectivity, detecting eventual associated cpe and intracellular presence of viral RNA and protein. Finally, CVB infection was ameliorated by IFN-Iβ treatment. We propose this model as a valid tool for additional studies investigating potential mechanisms underlying CVB infection in cardiomyocytes or for use in drug testing.

Materials and Methods

Reagents

Fluorescein isothiocyanate (FITC)-conjugated anti-mouse IgG, FITC-conjugated anti-rabbit IgG, Texas Red-X (TR)-conjugated anti-rabbit IgG, TR-conjugated anti-mouse IgG and 4,6-diamidino-2-fenilindol (DAPI) were purchased from Molecular Probes/Invitrogen (Carlsbad, CA). Murine monoclonal antibodies (mAb) anti-SSEA4 (clone 813-70), anti-Tra-1-60 (TRA-1-60), anti-Oct-3/4 (clone C-10), anti-GATA-4 (clone G-4) and anti-cardiac Troponin T (clone CT3) were purchased from Santa Cruz Biotechnology (Santa Cruz, CA). The mAb anti-DAF (clone IA10) was purchased from Pharmingen (San Diego, CA). The rabbit polyclonal anti-Nanog (clone H-155), anti-ANP (clone FL-153), anti-Nkx2.5 (clone H-114) and anti-CAR were purchased from Santa Cruz Biotechnology. Recombinant human IFN-Iß was obtained from InvivoGen (San Diego, CA). Random hexamers, SuperScript III reverse transcriptase, Trizol, DMEM and knock-out serum replacement (KSR) were from Invitrogen. Matrigel™ was from BD Bioscience (San Jose, CA). The basic fibroblast growth factor (bFGF) was purchase from R&D Systems (Minneapolis, MN). All of the other reagents were obtained from Sigma Chemical Co. (St. Louis, MO).

Cell lines and culture

The human embryonic stem cell (hESC) line WAO9 was purchased from WiCell Research Institute (WI), and the hESC

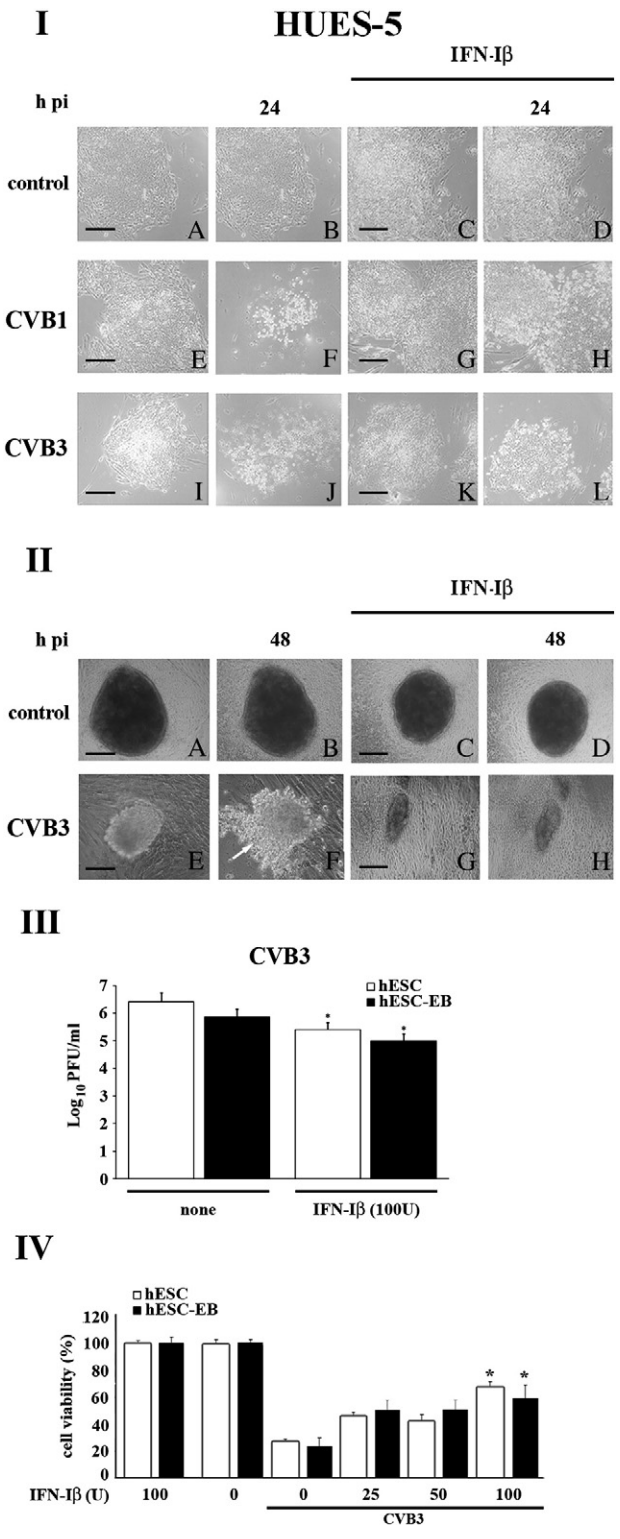

Figure 5 IFN-Iβ treatment reduced virus replication and cell death of infected cultured hESC and hESC-EB. (I) Representative images of HUES-5 hESC incubated with 100 units of IFN-Iβ 24 h prior to and during virus infection. The figure shows colonies control cells (A-B), control cells treated with IFN -Iβ (C-D), infected with CVB1 (E-F), treated with INF-Iβ and infected with CVB1 (G-H), infected with CVB3 (I-J) and treated with IFN-Iβ and infected with CVB3 (K-L). The scale bars represent 200 μm. (II) Representative images of HUES-5 hESC-EB incubated with 100 units of IFN-Iβ 24 h prior to and during virus infection. The figure shows colonies control EB (A-B), control EB treated with IFN -Iβ (C-D), infected with CVB3 (E-F), and treated with IFN-Iβ and infected with CVB3 (G-H). Arrow shows CVB3-related cpe in contractile areas. (III) Infectivity titration of infected cell supernatants performed with 100 μl of 10-fold serial dilutions in a plaque forming unit (PFU) assay at 24 h pi (hESC) or 48 h pi (hESC-EB) with or without IFN-Iβ treatment. (IV) Cell viability was measured by using the XTT/PMS vital dye assay at 24 h pi of hESC or 48 h pi of hESC-EB untreated or treated with 25 to 100 U of IFN-Iβ 24 h prior to and during virus infection. Each bar represents the mean ± SEM of two independent experiments (*$P<0.05$). Abbreviations: IFN-Iβ, Type I Interferon β; CVB1, Coxsackievirus subgroup B, serotype 1; CVB3, Coxsackievirus subgroup B, serotype 3.

lines HUES-5 and HUES-16 were acquired from Harvard University and the Howard Hughes Medical Institute (MA) at low passages (p15 to p20). The hESC lines were maintained on an inactivated mouse embryonic fibroblast (MEF) feeder layer in medium comprised of Dulbecco's Modified Eagle's Medium/Ham's F12 (DMEM/F12) supplemented with KSR 20% 2 mM non-essential amino acids, 2 mM L-glutamine, 100 U/ml penicillin, 50 μg/ml streptomycin, 0.1 mM β-mercaptoethanol and 4 ng/ml of bFGF on diluted (1/40) Matrigel™ coated dishes in MEF-conditioned medium. For the conditioning medium, 3×10^6 inactivated MEF cells were incubated for 24 h with 25 ml of DMEM/F12 medium supplemented with 5% KSR and 2 ng/ml of bFGF (in addition to the other aforementioned supplements) and stored at -20 °C. After thawing, fresh aliquots of KSR and bFGF were added to the medium to render a final concentration of 20% and 4 ng/ml, respectively.

To induce differentiation, hESC colonies were dispersed with 1 mg/ml of collagenase IV (Invitrogen) for 5 min. The cells were then transferred to non-adherent Petri dishes containing DMEM supplemented with 20% (vol/vol) fetal bovine serum (FBS, Gibco), 2 mM L-glutamine, 100 U/ml penicillin and 50 μg/ml streptomycin used as differentiation medium. The cells were incubated in suspension at 37 °C with 5% CO_2 for 7 days. During the incubation the cells aggregated to form EB, which were then plated on to 0.1% gelatin coated 24-well microplates and cultured for an additional 7 days. Normally, within the first 2-4 days after plating, contracting areas were observed in the outgrowth of the EB.

The HeLa cells that were used for transfections, virus propagation and viral titrations were obtained from ABAC (*Asociación Banco Argentino de Células, Argentina*) and were maintained as monolayers in MEM supplemented with 10% (vol/vol) FBS, 2 mM L-glutamine, 25.5 mM sodium bicarbonate and 50 μg of gentamicin/ml.

Virus

A CVB1 derived from an infectious cDNA clone has been previously described (Iizuka et al., 1991), as well as a myocarditic strain of CVB3 (Gomez et al., 1991, 1993). CVB2, CVB4 and CVB5 were obtained from the American Tissue Culture Collection (ATCC). The viral stocks were prepared by partially purifying the virus through a 30% sucrose cushion, as previously described (Rinehart et al., 1997).

Cell infection

The cells were infected at undifferentiated (day 0, hESC) or differentiated (day 14, hESC-EB) stages with a multiplicity of infection (MOI) of 1 for 1 h at 37 °C. Mock infection was performed by replacing the same volume of virus inoculum with HeLa cell supernatant from uninfected cells. The cells were then washed and maintained in conditioned medium or differentiation medium as needed.

Infectivity titration

The infectivity titration was performed with 100 μl of 10-fold serial dilutions of infected cell supernatants as previously described (Gomez et al., 1991).

Immunostaining and fluorescence microscopy

The hESC or hESC-EB were analyzed for *in situ* immunofluorescence. Briefly, the cells were rinsed with ice-cold PBS and fixed in PBSA (PBS with 0.1% bovine serum albumin) with 4% formaldehyde for 45 min. After two washes cells were permeabilized with 0.1% Triton X-100 in PBSA with 10% normal goat serum for 30 min, washed twice and stained with the corresponding primary antibodies. Fluorescent secondary antibodies were used to localize the antigen/primary antibody complexes. The cells were counterstained with DAPI and examined under a Nikon Eclipse TE2000-S inverted microscope equipped with a 20X E-Plan objective and a super high-pressure mercury lamp. The images were acquired with a Nikon DXN1200F digital camera, which was controlled by the EclipseNet software (version 1.20.0 build 61).

RNA isolation and RT-PCR

Total RNA was isolated from hESC or from contractile areas of hESC-EB by mechanical scraping with a scalpel under microscope and Trizol, as recommended by the manufacturer. DNase treatment was performed with an RNase-free DNase Kit (Qiagen). cDNA was synthesized from 500 ng of total RNA with 15 mM of random hexamers and SuperScript III reverse transcriptase, according to manufacturer's instructions. The cDNA samples were diluted 10-fold, and the PCR reaction was conducted at an annealing temperature of 55 °C. All of the reactions were within the linear range of amplification. For the real-time PCR studies, PCR amplification and analysis were performed with a Line-Gene instrument (Bioer). The TAQurate green real-time PCR MasterMix (Epicentre Biotechnologies) was used for all reactions, following manufacturer instructions. A melting curve analysis was performed immediately after amplification at a linear temperature transition rate of 0.3 °C/s from 70 °C to 89 °C with continuous fluorescence acquisition. After real-time PCR, the amplicon size was confirmed by gel electrophoresis. The primers sequences and sizes of the amplified fragments are shown in Table 1.

Cell viability assay

hESC were plated onto matrigel coated 96-well tissue culture plates at densities between $1\times10^4 - 3\times10^4$ cells per well and grown until confluence. After 7 days of suspension culture, individual EBs were plated onto 0.1% gelatin coated 96-well microplates and cultured for an additional 7 days as previously described. 24 h pi (hESC) or 48 h pi (contractile EB), 50 μg/well of activated 2,3-bis (2-methoxy-4-nitro-5-sulfophenyl)-5 [(phenylamino) carbonyl]-2 H-tetrazolium hydroxide (XTT) in PBS containing 0.3 μg/well of the intermediate electron carrier, N-methyl dibenzopyrazine methyl sulfate (PMS) were added (final volume 100 μl) and incubated for 1-2 h. Cellular metabolic activity was determined by measuring the absorbance of the samples with a spectrophotometer (ELISA reader) at a wavelength of 450 nm and subtracting the background absorbance at 690 nm.

Table 1 Primers used for the PCR experiments and size of amplified fragments

Gene	Fragment size	*Primers sequence (5´-3´)*	
		Forward	Reverse
Oct -4	126	CTGGGTTGATCCTCGGACCT	CACAGAACTCATACGGCGGG
Nanog	109	AAAGAATCTTCACCTATGCC	GAAGGAAGAGGAGAGACAGT
GATA-4	218	CATCAAGACGGAGCCTGGCC	TGACTGTCGGCCAAGACCAG
GATA-6	213	CCATGACTCCAACTTCCACC	ACGGAGGACGTGACTTCGGC
c-myc	109	ATGAAAAGGCCCCCAAGGTAG	CGTTTCCGCAACAAGTCCTCT
cTnT	107	ATGATGCATTTTGGGGGTTA	CAGCACCTTCCTCCTCTCAG
MESP1	111	TGAGGAGCCCAAGTGACAA	CTCTTCCAGGAAAGGCAGTCT
α-MHC	413	GTCATTGCTGAAACCGAGAATG	GCAAAGTACTGGATGACACGCT
Isl-1	201	CACAAGCGTCTCGGGATTGTGTTT	AGTGGCAAGTCTTCCGACAA
ß-actin	125	CAATGTGGCCGAGGACTTTG	CATTCTCCTTAGAGAGAAGTGG
CAR	293	AGTCCCGAAGACCAGGGACC	ACCTGAAGGCTTAACAAGAA
DAF	82	AATGGTCCACAGCAGTCGAAT	GGTACATCAATCTGACCATTTCGTA
IFNAR1	326	GTGATACACATCTCTCCTGG	GTATAATCCCATTTAAGAACATG
IFNAR2	394	GAGTAAACCAGAAGATTTGAAG	CGTGTTTGGAATTAACTTGTC
GAPDH	98	ACAGCCTCAAGATCATCAG	GAGTCCTTCCACGATACC
Entero	115	CGGCCCCTGAATGCGGCTAA	GAAACACGGACACCCAAAGTA

Statistical analysis

All of the results are expressed as the mean ± SEM. The student's paired *t* test was used to determine significant differences between means, and *P* values below 0.05 were considered to be statistically significant.

Supplementary materials related to this article can be found online at doi:10.1016/j.scr.2010.09.002.

Disclosures

None declared.

Acknowledgments

This work was supported by grants from Agencia Nacional de Promoción Científica y Tecnológica (ANPCyT) PID2007-00112, PICT 07-00642 and PICT 07-00028. CB, CJG, MQ and GVR are Graduate fellows. LR and MFF are post-doctoral fellows. SGM and RMG are Research Members of Consejo Nacional de Investigaciones Científicas y Técnicas (CONICET). The authors would like to thank Damian D. Fernandez Espinosa for his skillful technical assistance.

References

Anon, 2008. Increased detections and severe neonatal disease associated with coxsackievirus B1 infection—United States. MMWR Morb Mortal Wkly Rep 57, 553—556.

Bergelson, J.M., Cunningham, J.A., Droguett, G., Kurt-Jones, E.A., Krithivas, A., Hong, J.S., Horwitz, M.S., Crowell, R.L., Finberg, R.W., 1997. Isolation of a common receptor for Coxsackie B viruses and adenoviruses 2 and 5. Science 275, 1320—1323.

Brokhman, I., Pomp, O., Fishman, L., Tennenbaum, T., Amit, M., Itzkovitz-Eldor, J., Goldstein, R.S., 2009. Genetic modification of human embryonic stem cells with adenoviral vectors: differences of infectability between lines and correlation of infectability with expression of the coxsackie and adenovirus receptor. Stem Cells Dev. 18, 447—456.

Coyne, C.B., Bergelson, J.M., 2006. Virus-induced Abl and Fyn kinase signals permit coxsackievirus entry through epithelial tight junctions. Cell 124, 119—131.

Deonarain, R., Cerullo, D., Fuse, K., Liu, P.P., Fish, E.N., 2004. Protective role for interferon-beta in coxsackievirus B3 infection. Circulation 110, 3540—3543.

Ellis, C.R., Di Salvo, T., 2007. Myocarditis: basic and clinical aspects. Cardiol. Rev. 15, 170—177.

Feldman, A.M., McNamara, D., 2000. Myocarditis. N Engl J. Med. 343, 1388—1398.

Feuer, R., Mena, I., Pagarigan, R.R., Harkins, S., Hassett, D.E., Whitton, J.L., 2003. Coxsackievirus B3 and the neonatal CNS: the roles of stem cells, developing neurons, and apoptosis in infection, viral dissemination, and disease. Am. J. Pathol. 163, 1379—1393.

Feuer, R., Pagarigan, R.R., Harkins, S., Liu, F., Hunziker, I.P., Whitton, J.L., 2005. Coxsackievirus targets proliferating neuronal progenitor cells in the neonatal CNS. J. Neurosci. 25, 2434—2444.

Freimuth, P., Philipson, L., Carson, S.D., 2008. The coxsackievirus and adenovirus receptor. Curr. Top. Microbiol. Immunol. 323, 67—87.

Gomez, R.M., Lascano, E.F., Berria, M.I., 1991. Murine acinar pancreatitis preceding necrotizing myocarditis after Coxsackievirus B3 inoculation. J. Med. Virol. 35, 71—75.

Gomez, R.M., Cui, X., Castagnino, C.G., Berria, M.I., 1993. Differential behaviour in pancreas and heart of two coxsackievirus B3 variants. Intervirology 36, 153—160.

He, J.Q., Ma, Y., Lee, Y., Thomson, J.A., Kamp, T.J., 2003. Human embryonic stem cells develop into multiple types of cardiac myocytes: action potential characterization. Circ. Res. 93, 32—39.

Iizuka, N., Yonekawa, H., Nomoto, A., 1991. Nucleotide sequences important for translation initiation of enterovirus RNA. J. Virol. 65, 4867—4873.

Kandolf, R., Canu, A., Hofschneider, P.H., 1985. Coxsackie B3 virus can replicate in cultured human foetal heart cells and is inhibited by interferon. J. Mol. Cell. Cardiol. 17, 167—181.

Kehat, I., Kenyagin-Karsenti, D., Snir, M., Segev, H., Amit, M., Gepstein, A., Livne, E., Binah, O., Itskovitz-Eldor, J., Gepstein, L., 2001. Human embryonic stem cells can differentiate into myocytes with structural and functional properties of cardiomyocytes. J. Clin. Invest. 108, 407—414.

Kuhl, U., Pauschinger, M., Schwimmbeck, P.L., Seeberg, B., Lober, C., Noutsias, M., Poller, W., Schultheiss, H.P., 2003. Interferon-beta treatment eliminates cardiotropic viruses and improves left ventricular function in patients with myocardial persistence of viral genomes and left ventricular dysfunction. Circulation 107, 2793–2798.

Lev, S., Kehat, I., Gepstein, L., 2005. Differentiation pathways in human embryonic stem cell-derived cardiomyocytes. Ann. NY Acad. Sci. 1047, 50–65.

Li, Y., Bourlet, T., Andreoletti, L., Mosnier, J.F., Peng, T., Yang, Y., Archard, L.C., Pozzetto, B., Zhang, H., 2000. Enteroviral capsid protein VP1 is present in myocardial tissues from some patients with myocarditis or dilated cardiomyopathy. Circulation 101, 231–234.

Matsumori, A., 2007. Treatment options in myocarditis: what we know from experimental data and how it translates to clinical trials. Herz 32, 452–456.

Milstone, A.M., Petrella, J., Sanchez, M.D., Mahmud, M., Whitbeck, J.C., Bergelson, J.M., 2005. Interaction with coxsackievirus and adenovirus receptor, but not with decay-accelerating factor (DAF), induces A-particle formation in a DAF-binding coxsackievirus B3 isolate. J. Virol. 79, 655–660.

Noutsias, M., Fechner, H., de Jonge, H., Wang, X., Dekkers, D., Houtsmuller, A.B., Pauschinger, M., Bergelson, J., Warraich, R., Yacoub, M., Hetzer, R., Lamers, J., Schultheiss, H.P., Poller, W., 2001. Human coxsackie-adenovirus receptor is colocalized with integrins alpha(v)beta(3) and alpha(v)beta(5) on the cardiomyocyte sarcolemma and upregulated in dilated cardiomyopathy: implications for cardiotropic viral infections. Circulation 104, 275–280.

Pallansch, M.A., Roos, R.P., 2001. Enteroviruses: Polioviruses, Coxsackieviruses, Echoviruses, and Newer Enteroviruses. In: Fields, B.N., Howley, P.M., Griffin, D.E., Lamb, R.A., Martin, M.A., Roizman, B., Straus, S.E., Knipe, D.M. (Eds.), Virology. Lippincott Williams & Wilkins, Philadelphia, pp. 589–630.

Patel, K.P., Coyne, C.B., Bergelson, J.M., 2009. Dynamin- and lipid Raft-dependent entry of decay-accelerating factor (DAF)-binding and non-DAF-binding coxsackieviruses into nonpolarized cells. J. Virol. 83, 11064–11077.

Reppel, M., Igelmund, P., Egert, U., Juchelka, F., Hescheler, J., Drobinskaya, I., 2007. Effect of cardioactive drugs on action potential generation and propagation in embryonic stem cell-derived cardiomyocytes. Cell. Physiol. Biochem. 19, 213–224.

Rinehart, J.E., Gomez, R.M., Roos, R.P., 1997. Molecular determinants for virulence in coxsackievirus B1 infection. J. Virol. 71, 3986–3991.

Shafren, D.R., Bates, R.C., Agrez, M.V., Herd, R.L., Burns, G.F., Barry, R.D., 1995. Coxsackieviruses B1, B3, and B5 use decay accelerating factor as a receptor for cell attachment. J. Virol. 69, 3873–3877.

Spiller, O.B., Goodfellow, I.G., Evans, D.J., Almond, J.W., Morgan, B.P., 2000. Echoviruses and coxsackie B viruses that use human decay-accelerating factor (DAF) as a receptor do not bind the rodent analogues of DAF. J. Infect. Dis. 181, 340–343.

Stanway, G., Brown, F., Christian, P., Hovi, T., Hyypiä, T., King, A.M.Q., Knowles, N.J., Lemon, S.M., Minor, P.D., Pallansch, M.A., Palmenberg, A.C., Skern, T., 2004. Picornaviridae. In: Fauquet, C.M., Mayo, M.A., Maniloff, J., Desselberger, U., Ball, L.A. (Eds.), Virus taxonomy. VIIIth Report of the ICTV, Elsevier, London, United Kingdom, pp. 757–778.

Steel, D., Hyllner, J., Sartipy, P., 2009. Cardiomyocytes derived from human embryonic stem cells - characteristics and utility for drug discovery. Curr. Opin. Drug Discov. Devel. 12, 133–140.

Tabor-Godwin, J.M., Ruller, C.M., Bagalso, N., An, N., Pagarigan, R.R., Harkins, S., Gilbert, P.E., Kiosses, W.B., Gude, N.A., Cornell, C.T., Doran, K.S., Sussman, M.A., Whitton, J.L., Feuer, R., 2010. A novel population of myeloid cells responding to coxsackievirus infection assists in the dissemination of virus within the neonatal CNS. J. Neurosci. 30, 8676–8691.

Thomson, J.A., Itskovitz-Eldor, J., Shapiro, S.S., Waknitz, M.A., Swiergiel, J.J., Marshall, V.S., Jones, J.M., 1998. Embryonic stem cell lines derived from human blastocysts. Science 282, 1145–1147.

Tracy, S., Gauntt, C., 2008. Group B coxsackievirus virulence. Curr. Top. Microbiol. Immunol. 323, 49–63.

Xu, C., Police, S., Rao, N., Carpenter, M.K., 2002. Characterization and enrichment of cardiomyocytes derived from human embryonic stem cells. Circ. Res. 91, 501–508.

Yajima, T., Knowlton, K.U., 2009. Viral myocarditis: from the perspective of the virus. Circulation 119, 2615–2624.

Yokoo, N., Baba, S., Kaichi, S., Niwa, A., Mima, T., Doi, H., Yamanaka, S., Nakahata, T., Heike, T., 2009. The effects of cardioactive drugs on cardiomyocytes derived from human induced pluripotent stem cells. Biochem. Biophys. Res. Commun. 387, 482–488.

Zhang, J., Wilson, G.F., Soerens, A.G., Koonce, C.H., Yu, J., Palecek, S.P., Thomson, J.A., Kamp, T.J., 2009. Functional cardiomyocytes derived from human induced pluripotent stem cells. Circ. Res. 104, e30–e41.

Zhong, Z., Li, X., Zhao, W., Tong, L., Liu, J., Wu, S., Lin, L., Zhang, Z., Tian, Y., Zhang, F., 2008. Mutations at nucleotides 573 and 579 within 5'-untranslated region augment the virulence of coxsackievirus B1. Virus Res. 135, 255–259.

Zimmermann, A., Gerber, H., Nussenzweig, V., Isliker, H., 1990. Decay-accelerating factor in the cardiomyocytes of normal individuals and patients with myocardial infarction. Virchows Arch. A Pathol. Anat. Histopathol. 417, 299–304.